Thermal and Mechanical Properties of Poly(butylene succinate) Nanocomposites with Various Organo-Modified Montmorillonites

Yoshihiro Someya, Toshiyuki Nakazato, Naozumi Teramoto, Mitsuhiro Shibata

Department of Industrial Chemistry, Faculty of Engineering, Chiba Institute of Technology, 2-17-1, Tsudanuma, Narashino, Chiba 275-0016, Japan

Received 12 March 2003; accepted 16 June 2003

ABSTRACT: Nanocomposites based on biodegradable poly(butylene succinate) (PBS) and layered silicates were prepared by melt intercalation. Nonmodified montmorillonite (MMT) and MMTs (DA-M, ODA-M, ALA-M, LEA-M, and HEA-M) organo-modified by protonated ammonium cations {i.e., those of dodecylamine, octadecylamine, 12-aminolauric acid, *N*-lauryldiethanolamine, and 1-[*N*,*N*-bis(2-hydroxyethyl)amino]-2-propanol, respectively} were used as layered silicates. From morphological studies using transmission electron microscopy, DA-M, ODA-M, and LEA-M were found to be dispersed homogeneously in the matrix polymer, whereas some clusters or agglomerated particles were observed for ALA-M, HEA-M, and MMT. The enlargement of the difference in the interlayer spacing between the clay and PBS/clay composite, as measured by X-ray diffraction, had a good correlation with the improvement of the clay dispersion and with the increase in the tensile modulus and the decrease in the tensile strength of the PBS composites with an inorganic concentration of 3 wt %. Dynamic viscoelastic measurements of the PBS/LEA-M nanocomposite revealed that the storage modulus and glass-transition temperature increased with the inorganic concentration (3–10 wt %). © 2003 Wiley Periodicals, Inc. J Appl Polym Sci 91: 1463–1475, 2004

Key words: nanocomposites; biodegradable; polyesters; organoclay; mechanical properties

INTRODUCTION

Biodegradable plastics, such as aliphatic polyesters, cellulose-based thermoplastics, and other polysaccharide-based plastics, have been extensively investigated, since the 1970s, in an attempt to reduce the environmental pollution caused by plastic wastes.[1,2] Among biodegradable plastics, most of the aliphatic polyesters, such as poly(ϵ-caprolactone) (PCL), poly(3-hydroxybutyrate-*co*-3-hydroxyvalerate),[3–6] and poly(butylene succinate) (PBS),[7,8] have lower mechanical strength and modulus values than poly(ethylene terephthalate), which is a conventional thermoplastic polyester. Recently, the reinforcement of such biodegradable polyesters with layered silicates (nanocomposites)[9–15] or natural fibers (biocomposites)[16–18] as environmentally benign materials has received significant research attention. In particular, the former nanocomposites have given rise to a steadily increasing interest among scientists and industrial researchers because they often exhibit greatly improved mechanical, thermal, barrier, and fire-retardant properties at low clay contents in comparison with more conventional microcomposites.[19–21] The nanocomposites can be prepared by four different methods: solution intercalation, *in situ* intercalative polymerization, polymer melt intercalation, and template synthesis.[22] Polymer melt intercalation has been proven to be an excellent technique because of its versatility, its compatibility with current polymer processing techniques, and its environmentally benign character due to the absence of any solvent.[23] A PBS nanocomposite prepared by melt intercalation with octadecylammonium-modified montmorillonite (MMT) has been reported to exhibit a higher storage modulus in dynamic viscoelastic measurements.[14] The objective of our research is to investigate the influence of the type of organoclay on the morphologies and thermal and mechanical properties of PBS nanocomposites. Our attention is focused on the relationship between the extent of intercalation and the mechanical properties.

Correspondence to: M. Shibata (shibata@pf.it-chiba.ac.jp).

Journal of Applied Polymer Science, Vol. 91, 1463–1475 (2004)

EXPERIMENTAL

Materials

PBS {Bionolle 1020; melt-flow rate (190°C, 2.16 kg) = 25 g/10 min, specific gravity = 1.26, glass-transition temperature (T_g) = −32°C [differential scanning calorimetry (DSC)], melting temperature (T_m) = 115°C

TABLE I
Synthetic Data and CER Values of Various Organoclays

Amine	HCl/amine molar ratio	Amine/exchangeable cation molar ratio	Organic fraction of organoclay (wt %)	CER (%)
DA	1.5	1.3	18.6	103.4
ODA	1.5	1.3	21.8	87.7
LEA	1.5	1.3	23.2	87.2
HEA	2.0	8.0	14.9	79.3
ALA	1.5	1.3	16.0	75.1

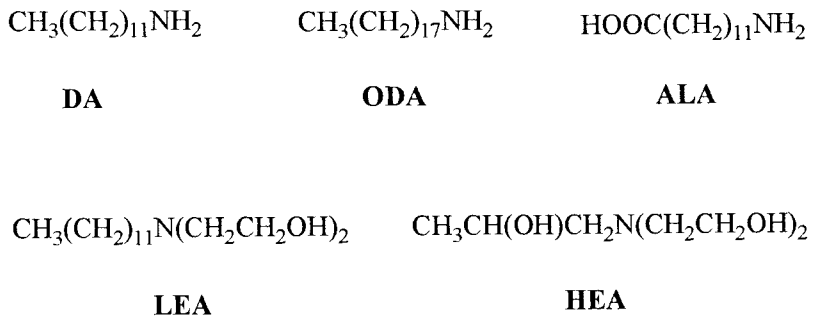

Figure 1 Amine compounds used for the preparation of the organoclays.

(DSC)} was supplied by Showa Highpolymer Co., Ltd. (Tokyo, Japan). Sodium (Na^+) MMT [Kunipia F; cation-exchange capacity (CEC) = 115 mequiv/100 g] was supplied by Kunimine Industries Co., Ltd. (Tokyo, Japan). The amines used for the preparation of the organophilic clays were dodecylamine (DA), octadecylamine (ODA), 12-aminolauric acid (ALA), *N*-lauryldiethanolamine (LEA), and 1-[*N*,*N*-bis(2-hydroxyethyl)amino]-2-propanol (HEA), which were supplied by Tokyo Kasei Kogyo Co., Ltd. (Tokyo, Japan). All the other chemicals used in this work were reagent-grade and were used without further purification.

Preparation of the organoclays

Each organoclay was prepared by the cation exchange of natural counterions with organic ammonium compounds. In all cases except HEA, the molar ratio of the exchangeable cation (calculated from the CEC value), the amine, and the hydrochloric acid was 1.0:1.3:1.95. A typical procedure for LEA was as follows: MMT (10.0 g, 11.5 mmol of the exchangeable cation) was dispersed in 1000 mL of deionized water at room temperature. LEA (4.09 g, 15.0 mmol) was dissolved in a mixture of deionized water (78 mL) and concentrated hydrochloric acid (1.93 mL, 22.4 mmol) and slowly poured into the clay suspension. The suspension was stirred for 1 h at 80°C. The exchanged clay was filtered, washed with a 1:1 mixture of water and ethanol, and redispersed in deionized water. This procedure was repeated several times until no chlorine ions were detected with a 0.14*N* $AgNO_3$ solution. The filter cake was freeze-dried, crushed into a powder with a mortar and pestle, and screened with a 280-mesh sieve. The LEA-modified MMT is denoted LEA-M.

The synthetic data and cation-exchange rates (CERs) of the organoclays are summarized in Table I.

Preparation of the composites

The sodium MMT and organoclay particles and PBS pellets were dried *in vacuo* at 40°C for at least 24 h before they were used. The melt mixing of PBS with the clay particles was performed on a Laboplasto-Mill with a twin rotary roller mixer (Toyo Seiki Co., Ltd., Tokyo, Japan). The inorganic concentration of the blends varied from 1.0 to 10.0 wt %. The mixing was carried out for 5 min at a rotary speed of 50 rpm at 140°C. The mixture was crushed into small pieces after immersion in liquid nitrogen, and it was dried at 40°C *in vacuo* for at least 24 h before injection molding. Each dumbbell-shaped specimen (5 mm wide, 2 mm thick, 32 mm long in its parallel part, and 72 mm long in all) was molded with a desk injection-molding machine (Little-Ace I Type, Tsubako Co., Ltd., Chigasaki, Japan). The cylinder temperature and molding temperature during the injection molding were 140 and 60°C, respectively.

Measurements

The CER values of the organoclays were calculated from the CEC value (115 mequiv/100 g) of Kunipia F and the weight decrease [W_1 (g)] and remaining weight [W_2 (g)] measured by thermogravimetric anal-

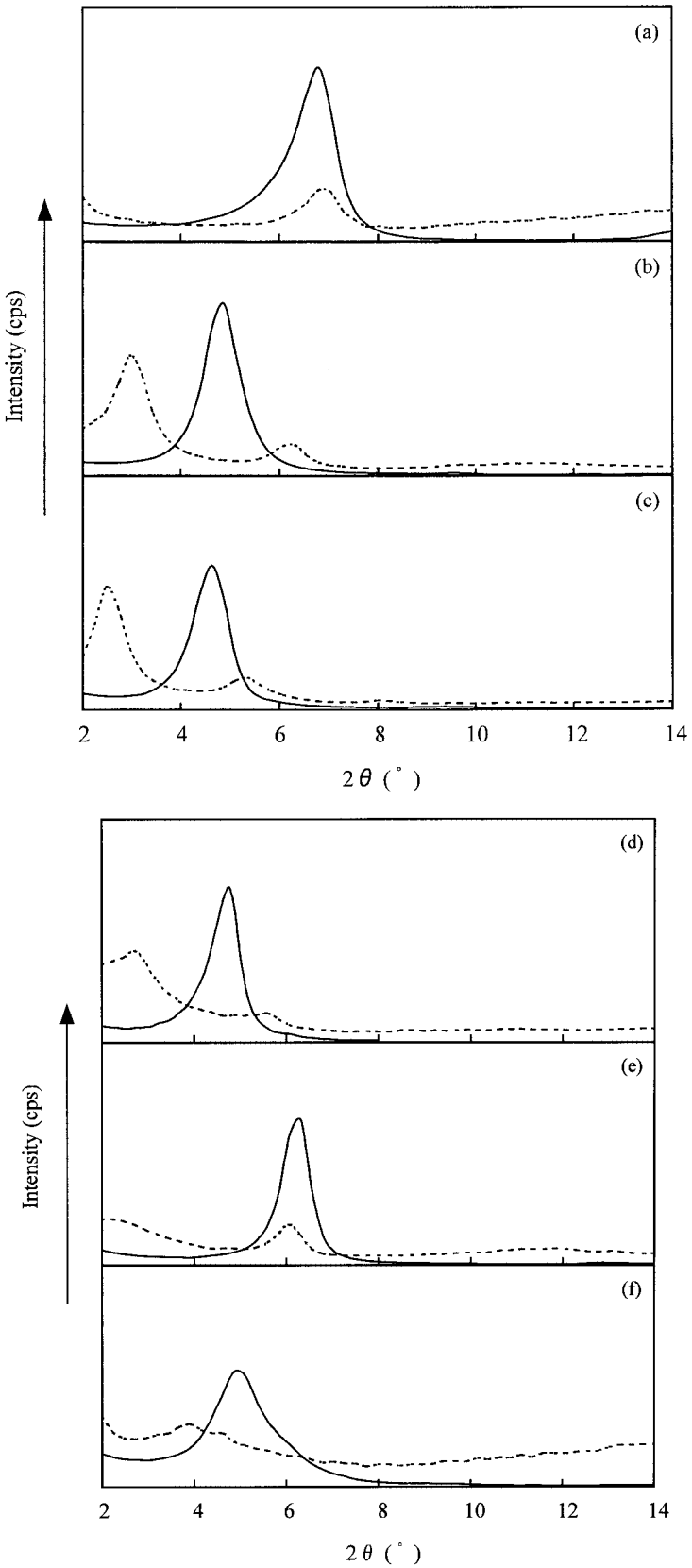

Figure 2 XRD patterns of (—) clays and (– – –) PBS/clay composites with an inorganic concentration of 3 wt %: (a) MMT and PBS/MMT, (b)DA-M and PBS/DA-M, (c)ODA-M and PBS/ODA-M, (d)LEA-M and PBS/LEA-M, (e) HEA-M and PBS/HEA-M, and (f) ALA and PBS/ALA-M.

TABLE II
Interlayer Spacing as Determined by XRD Analysis

Clay	XRD peak position (2θ)		Interlayer spacing [001] (nm)		
	In clay	In composite	In clay (d_1)	In composite (d_2)	Δd (nm)[a]
MMT	7.02	7.02	1.26	1.26	0.00
DA-M	5.00	3.20, 6.46[b]	1.77	2.76	0.99
ODA-M	4.84	2.70, 5.50[b]	1.82	3.27	1.45
LEA-M	4.86	2.72, 5.70[b]	1.82	3.25	1.43
HEA-M	6.46	6.30	1.37	1.40	0.03
ALA-M	5.16	3.68	1.71	2.21	0.50

[a] $\Delta d = d_2 - d_1$ (nm).
[b] The weak peak with a higher 2θ value was due to the [002] plane of the silicate layers.

ysis (TGA) on a PerkinElmer TGA-7 instrument (Yokohama, Japan) when the organoclays were heated from room temperature to 700°C at a heating rate of 20°C/min in a nitrogen atmosphere. CER was calculated as follows: CER (%) = $100(W_1/\mathrm{MW})/[10^{-5}\mathrm{CEC}(W_2 + 23.0W_1/\mathrm{MW})]$, where MW is the molecular weight of the organic ammonium cation. The organic fraction (wt %) of each organoclay was $100W_1/(W_1 + W_2)$.

Flexural and tensile tests of the composites were performed with an Autograph AGS-500C (Shimadzu Co., Ltd., Tokyo, Japan) according to the standard method for testing the flexural and tensile properties of plastics [JIS K7203 (1995) and K7113 (1995)]. The span length was 30 mm for flexural tests and 50 mm for tensile tests, and the testing speed was 10 mm/min. Five composite specimens were tested for each set of samples, and the mean values and standard deviation were calculated.

The X-ray diffraction (XRD) analysis was performed at the ambient temperature on a Rigaku RINT-2100 X-ray diffractometer (Tokyo, Japan) at a scanning rate of 2.0°/min with Cu Kα radiation (λ = 0.154 nm) at 40 kV and 14 mA. Sodium MMT and freeze-dried organoclays were studied as powders. The blended materials were prepared in films about 400 μm thick via compression molding.

Dynamic viscoelastic measurements of the films were obtained on a Rheolograph Solid (Toyo Seiki) with a chuck distance of 20 mm, a frequency of 10 Hz, and a heating rate of 2°C/min. Transmission electron microscopy (TEM) was performed on an electron microscope with a 75-kV accelerating voltage. The dumbbell-shaped samples were sectioned into roughly 100-nm thin sections at −70°C with a ultramicrotome with a diamond knife and then were mounted on 200-mesh copper grids.

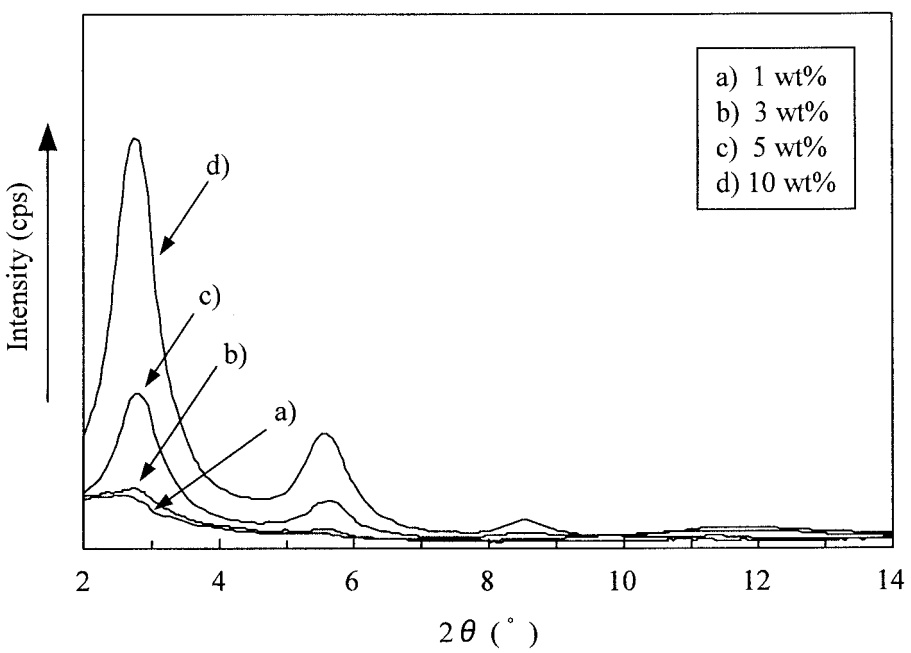

Figure 3 XRD patterns of PBS/LEA-M composites with various inorganic concentrations.

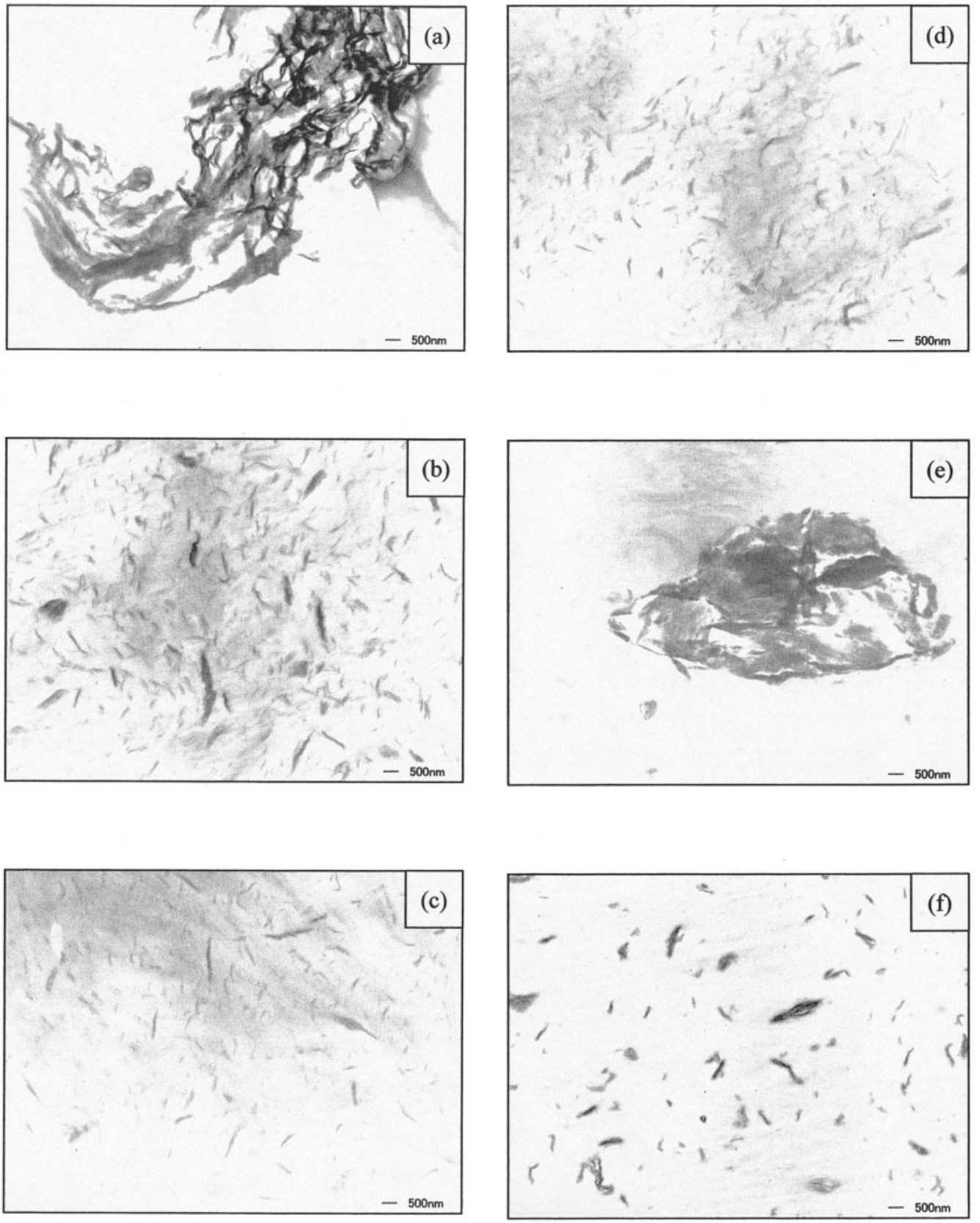

Figure 4 TEM images of PBS composites with an inorganic concentration of 3 wt %: (a) PBS/MMT, (b) PBS/DA-M, (c) PBS/ODA-M, (d) PBS/LEA-M, (e) PBS/HEA-M, and (f) PBS/ALA-M.

TABLE III
Mechanical Properties of PBS and PBS/Clay Composites with an Inorganic Content of 3 wt %

	Tensile properties			Flexural properties	
Clay	Strength (MPa)	Modulus (GPa)	Elongation at break (%)	Strength (MPa)	Modulus (GPa)
None	33.7	0.707	7.60	44.3	0.754
MMT	33.3	0.811	7.87	49.9	0.913
DA-M	31.3	1.013	6.32	49.6	1.096
ODA-M	30.8	1.002	6.34	48.4	1.025
LEA-M	29.7	1.044	6.30	48.6	1.036
HEA-M	33.5	0.836	6.99	44.6	0.774
ALA-M	32.2	0.857	6.37	45.1	0.807

DSC was performed on a PerkinElmer DSC Pyris 1 instrument in a nitrogen atmosphere. The crystallization temperature from the glassy state ($T_{g,c}$) and T_m of the PBS composite were determined from the first heating scan of the injection-molded sample at a heating rate of 10°C/min, and the crystallization temperature from the melt ($T_{m,c}$) was determined from the subsequent cooling process at a cooling rate of 10°C/min. A clear T_g was not observed for the heating and cooling processes.

RESULTS AND DISCUSSION

Dispersion of the organoclay in PBS

Five kinds of amine compounds, as shown in Figure 1 for the preparation of the organoclays, were selected to investigate the effects of variations in the hydrophobicity and polar/steric interactions on the nanostructures of the PBS hybrids. The solid lines shown in Figure 2 are XRD patterns of MMT and organoclays. The peaks correspond to the [001] basal reflection of the MMT aluminosilicate. From the angular location of the peaks and the Bragg condition, the interlayer spacing (d_1) of each of the clays was determined. The computed values are summarized in Table II. The difference in the interlayer spacing between the natural clay and organoclay is due to the intercalation of the ammonium surfactant. The surfactant with a bulkier substituent on the nitrogen atom shows a higher interlayer spacing. The dotted lines shown in Figure 2 are the XRD patterns of the PBS composites with an inorganic concentration of 3 wt %. The difference (Δd) in the interlayer spacing between the clay and PBS/clay is related to the degree of intercalation. The Δd value of PBS/MMT is zero, indicating that little or no intercalation occurred. All the PBS/organoclay composites, except for the PBS/HEA-M composite, had a Δd value larger than 0.4 nm, and this means that PBS is intercalated into the gallery of silicate layers to some extent. It is thought that HEA, having three small hydroxyalkyl groups, is not effective for the intercalation of PBS molecules. The PBS/ODA-M and PBS/LEA-M composites had the largest Δd value (1.4–1.5 nm), and this indicated that the extent of intercalation of the PBS molecule was the highest. In this case, two to three molecular layers may be intercalated if the PBS molecules are intercalated in the extended form because the approximate width of the extended molecular chain of PBS, according to Chem3D, is about 0.4–0.6 nm. Although we thought that terminal carboxylic groups could interact with the PBS molecule, ALA-M showed a lower value of Δd than DA-M with the same carbon number (C_{12}) as a result. For the PBS/LEA-M composites, the diffraction peak increased in intensity at the same position as the clay concentration increased from 1 to 10 wt % (see Fig. 3). This result means an increase in number of silicate layers with the same degree of intercalation.

Figure 4 shows TEM images of PBS composites with an inorganic concentration of 3 wt %. It is obvious that the order of the finer dispersion of the silicate particles in the PBS matrix is LEA-M, ODA-M > DA-M > ALA-M > HEA-M, MMT. The PBS/ODA-M and LEA-M composites showed a stacked intercalated structure, which was disorderly and uniformly dispersed in the PBS matrix, in agreement with the results of XRD. The presence of the exfoliated structure into single layers was not identified.

Mechanical properties of the PBS composites

Table III summarizes the tensile and flexural properties of the PBS composites. Figure 5 shows the relationship between Δd and the tensile properties. The tensile strength decreased with increasing Δd, and the tensile modulus increased with increasing Δd. However, we could not get a clear tendency for the relationship between Δd and the flexural properties (Fig. 6). A similar tendency between the extent of intercalation and the tensile properties was also observed for a PCL nanocomposite.[11] The reason is not clear, but it is thought that the increase in the tensile modulus is due to a better dispersion of silicate layers having a high modulus and a high aspect ratio, and the de-

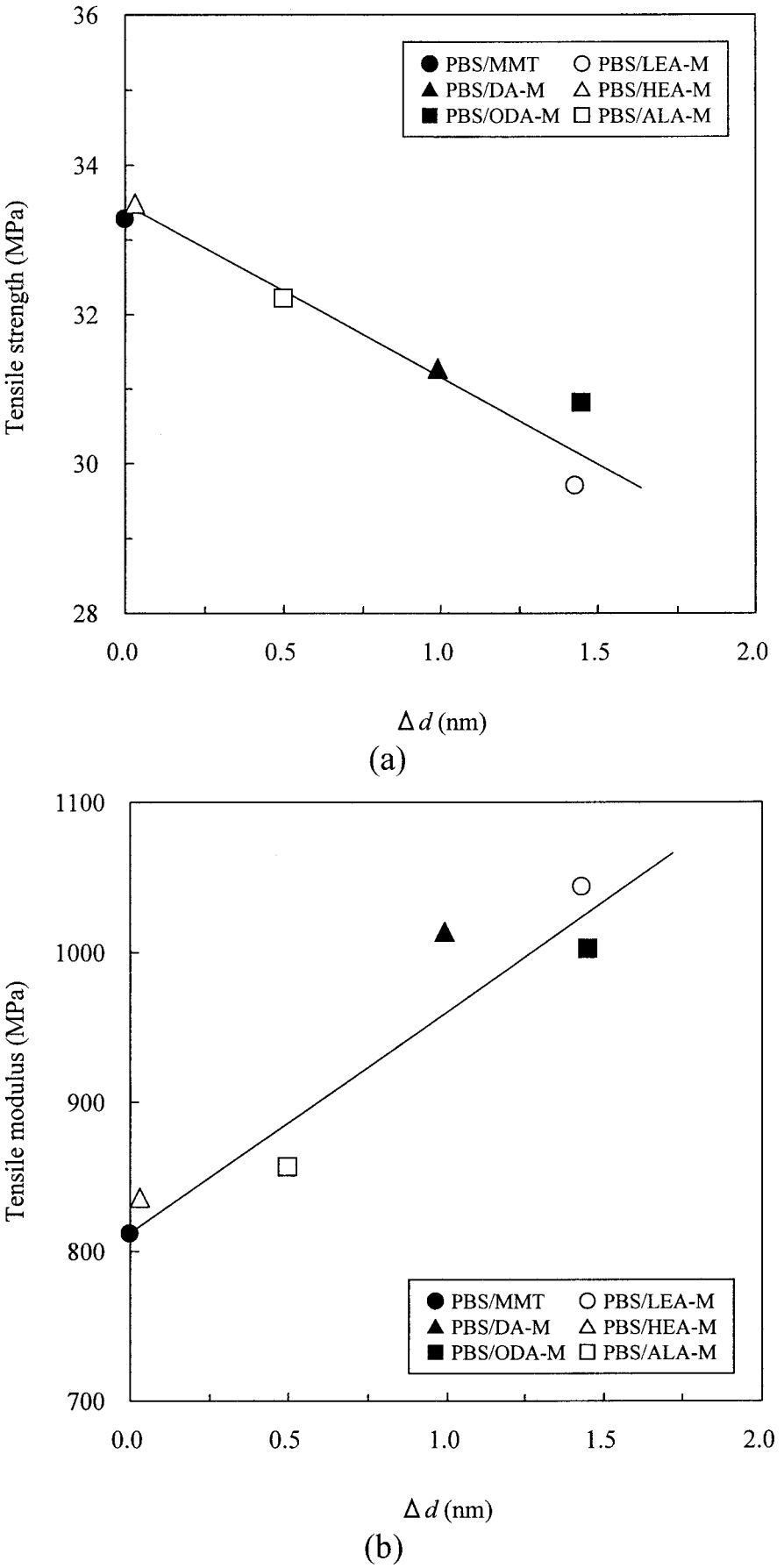

Figure 5 Relationship between Δd and the tensile properties of PBS composites with an inorganic concentration of 3 wt %: (a) the tensile strength and (b) the tensile modulus.

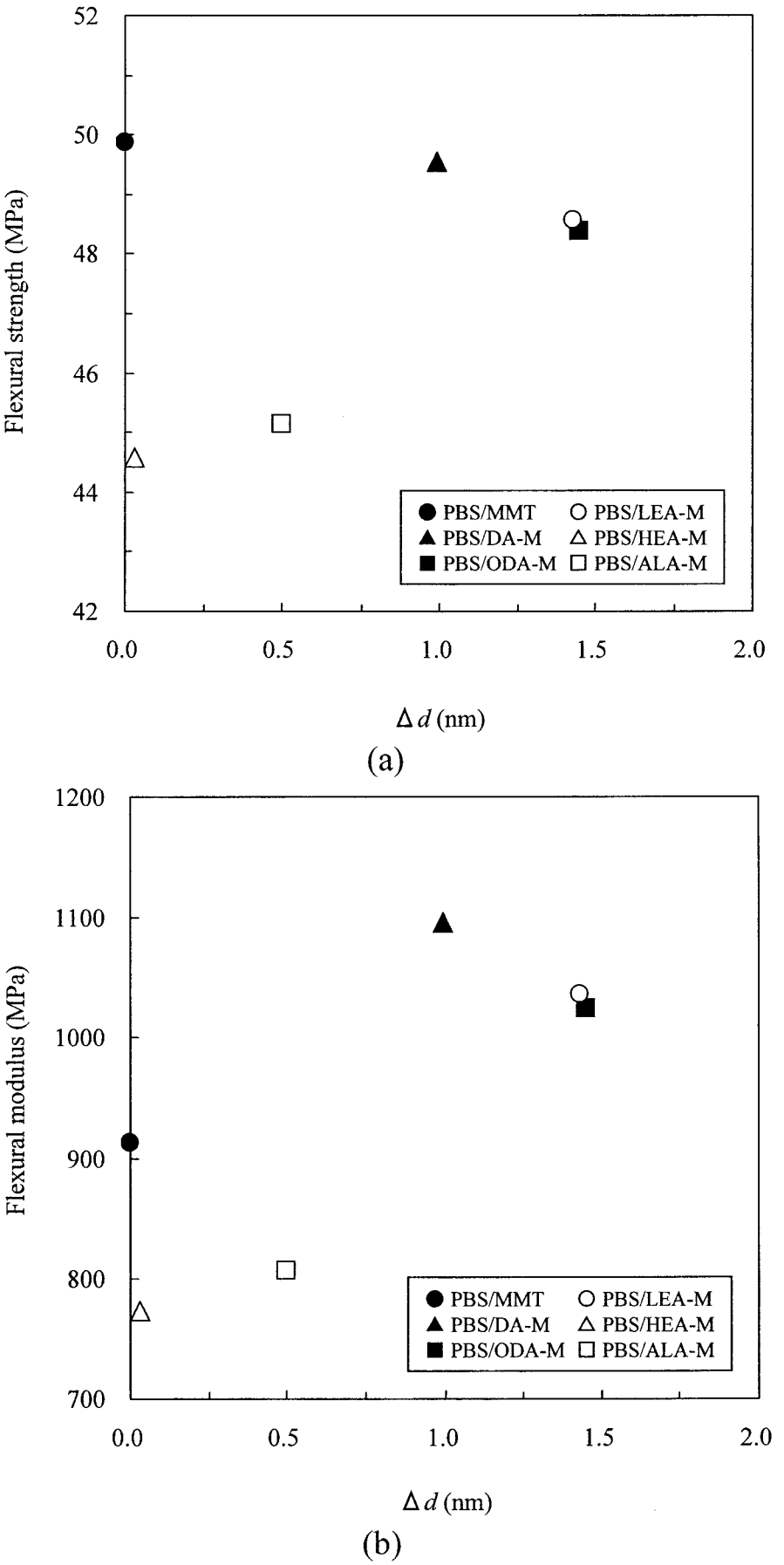

Figure 6 Relationship between Δd and the flexural properties of PBS composites with an inorganic concentration of 3 wt %: (a) the flexural strength and (b) the flexural modulus.

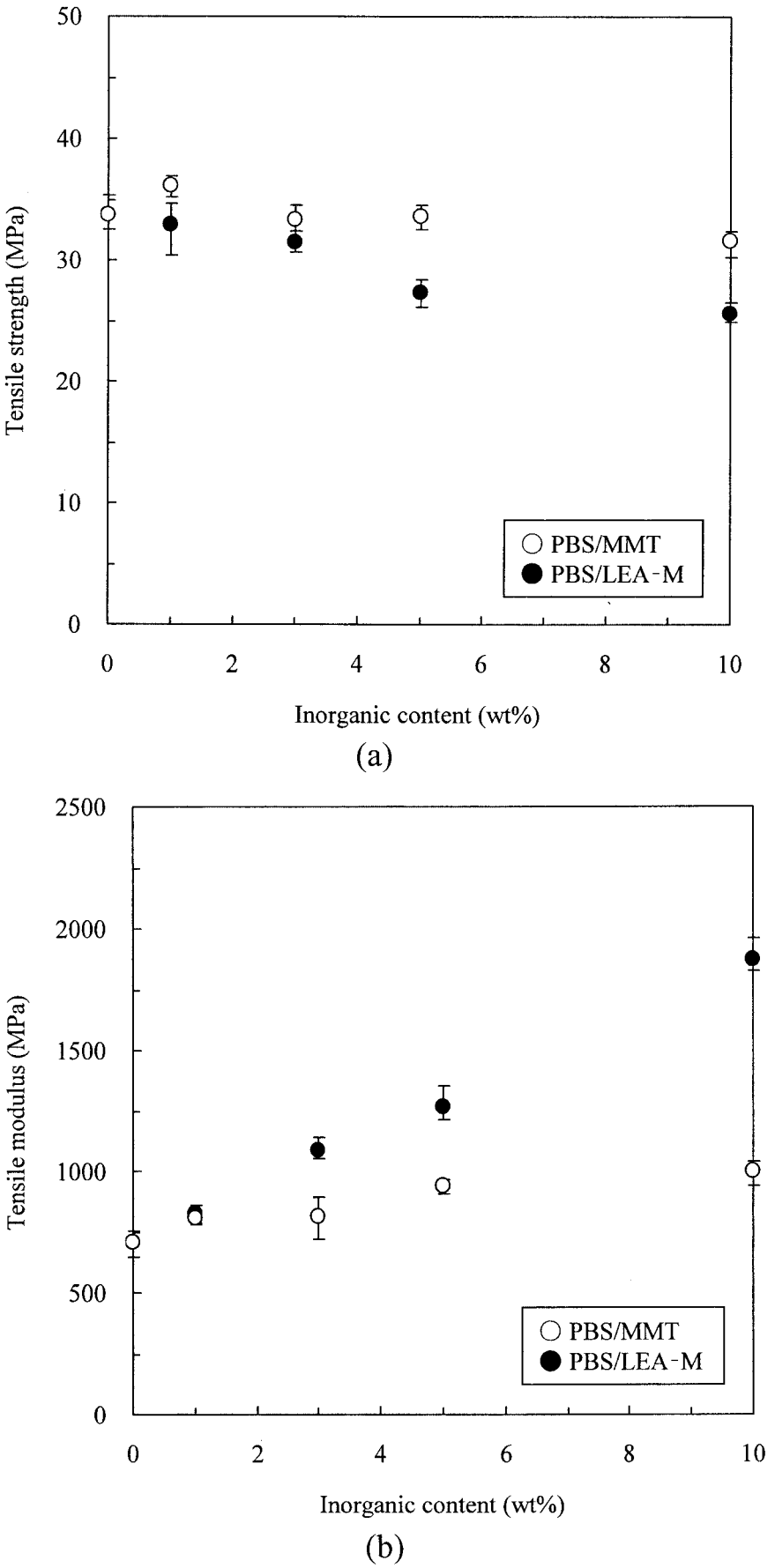

Figure 7 Tensile properties versus the inorganic concentration for PBS/MMT and PBS/LEA-M composites: (a) the tensile strength, (b) the tensile modulus, and (c) the elongation at break.

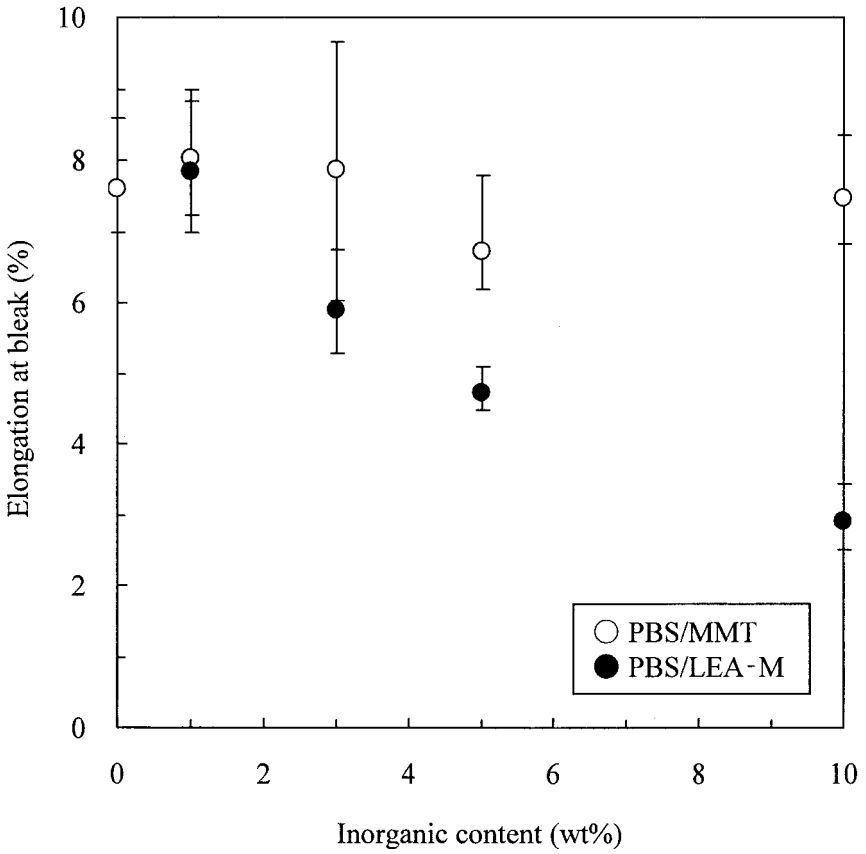

(c)

Figure 7 (*Continued from the previous page***)**

crease in the tensile strength is attributed to the decrease in the elongation at break, which is probably related to the delamination of the polymer–silicate interlayer. A higher degree of intercalation should cause a better dispersion of some exfoliated thin multilayer stacks into the matrix polymer, leading to an increase in the polymer–silicate interlayer. That a clear decreasing trend of the strength was not observed in the flexural mode may be attributed to the fact that the delamination did not significantly affect the strength because the flexural deformation was composed of both modes of compression and expansion (Fig. 6). Figure 7 shows the relationship between the tensile properties and inorganic content for PBS/MMT and

TABLE IV
Dynamic Viscoelastic Properties of PBS and PBS Composites

Sample	Inorganic content (wt %)	Storage modulus (GPa)			Tan δ peak temperature (°C)
		−60°C	−20°C	20°C	
PBS	0	2.06	1.09	0.59	−18.9
PBS/MMT	1	2.32	1.37	0.67	−15.0
PBS/MMT	3	2.13	1.15	0.63	−19.1
PBS/MMT	5	2.41	1.49	0.77	−15.0
PBS/MMT	10	2.44	1.53	0.79	−16.1
PBS/DA-M	3	2.36	1.36	0.72	−18.0
PBS/ODA-M	3	2.30	1.42	0.75	−18.9
PBS/LEA-M	1	2.12	1.30	0.63	−16.0
PBS/LEA-M	3	2.53	1.49	0.81	−20.1
PBS/LEA-M	5	2.63	1.78	1.02	−14.0
PBS/LEA-M	10	3.06	2.39	1.51	−4.2
PBS/HEA-M	3	2.40	1.40	0.67	−18.9
PBS/ALA-M	3	2.12	1.11	0.64	−20.0

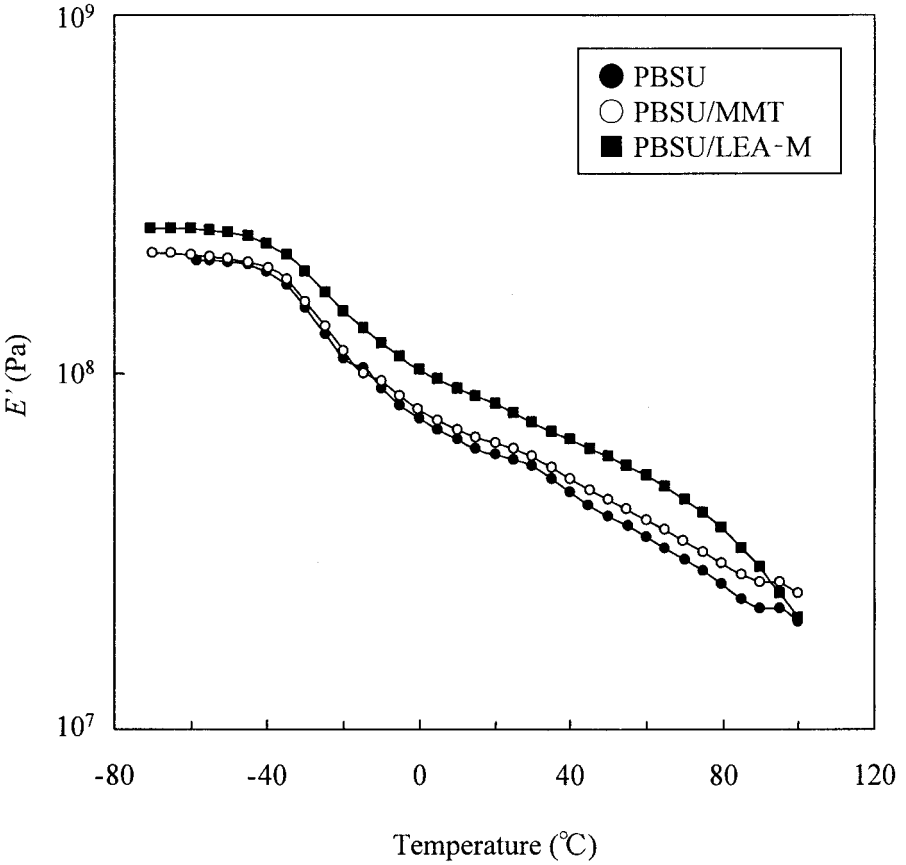

Figure 8 Temperature dependence of the storage modulus (E') for PBS and PBS/MMT and PBS/LEA-M composites with an inorganic concentration of 3 wt %.

PBS/LEA-M composites. With more than 1–10 wt % inorganic content, the PBS/LEA-M nanocomposite showed a higher tensile modulus and a lower tensile strength and elongation than the PBS/MMT composite. The tensile modulus of the PBS/LEA-M nanocomposite linearly increased with the clay content, but that of the PBS/MMT composite did not increase.

Dynamic viscoelastic properties of the PBS composites

Table IV summarizes the storage modulus and tan δ peak temperature measured by dynamic viscoelastic analysis for PBS and all the PBS composites. In agreement with the results for the tensile modulus, the PBS composite with a higher degree of intercalation showed a higher storage modulus over the temperature range of −60 to 90°C (Fig. 8). For the PBS/LEA-M nanocomposites, the storage modulus considerably increased with increasing inorganic content in comparison with that of the PBS/MMT composites. Furthermore, the tan δ peak temperature corresponding to T_g for the PBS/LEA-M composite considerably shifted to a higher temperature region with the inorganic content (Fig. 9). In particular, the PBS/LEA-M composite with an inorganic concentration of 10 wt % had a significantly higher T_g (−4.2°C) than PBS (−18.9°C). This result indicates that the intercalation of PBS into the galley of silicate layers caused the interference of the molecular motion. However, a small difference was observed in the tan δ peak temperature for the PBS/MMT composites.

Thermal properties of the PBS composites

The thermal properties of the PBS composites determined by DSC measurements are summarized in Table V. When we discuss the mechanical properties of PBS nanocomposites in connection with the degree of intercalation, the influence of the degree of crystallinity (χ_c) of the PBS component in the composites should be considered because χ_c may change with the influence of the organoclay. The original χ_c value of the injection-molded composite can be evaluated from the value of $\Delta H_m - \Delta H_{g,c}$, where ΔH_m and $\Delta H_{g,c}$ are the heat of melting and heat of crystallization from the glassy state of the injection-molded sample in the first heating DSC scan, respectively. The χ_c values of the injection-molded PBS/DA-M, ODA-M, LEA-M, and

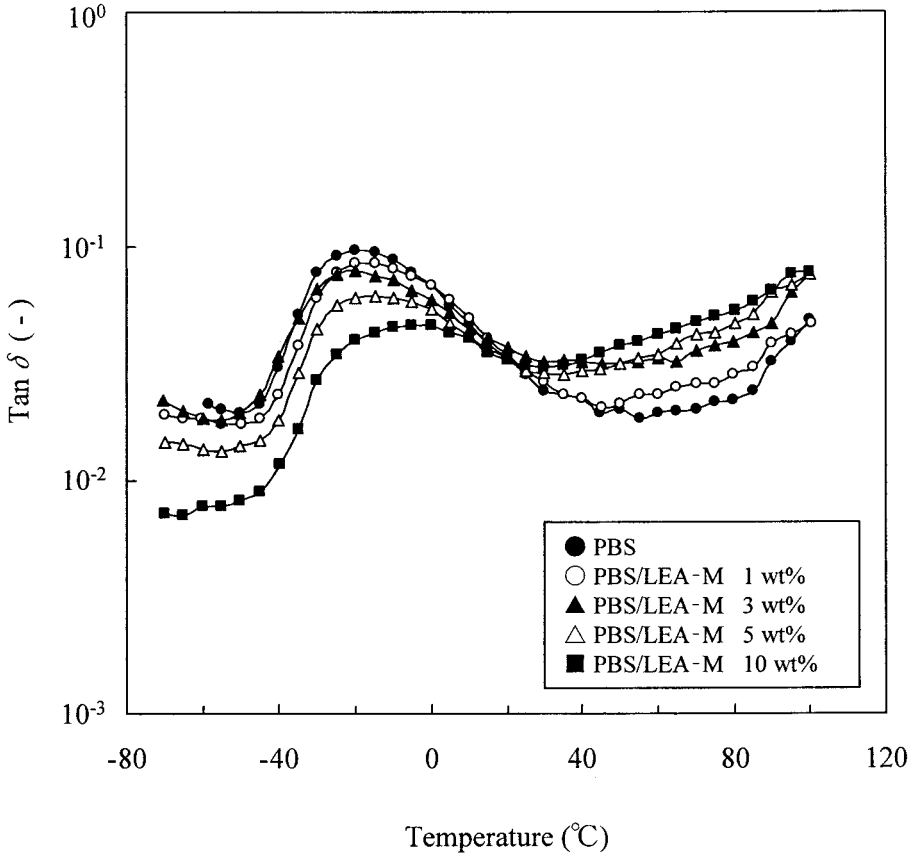

Figure 9 Temperature dependence of tan δ for PBS/LEA-M composites with various inorganic concentrations.

HEA-M samples were evaluated to be 93–94% of that of the PBS/MMT composite, on the basis of the $\Delta H_m - \Delta H_{g,c}$ value. The lower tensile strength of PBS/DA-M, ODA-M, and LEA-M should not be attributed to a χ_c value lower than that of PBS/MMT because PBS/HEA-M, having a relatively high tensile strength, showed a χ_c value similar to those of PBS/DA-M, ODA-M, and LEA-M. As a result, it is thought that the mechanical properties of the PBS composites are not seriously affected by a change in χ_c. All the PBS/clay composites showed higher $T_{m,c}$ values and heats of crystallization from the melt ($\Delta H_{m,c}$) than PBS, and this indicated that the crystallization from the melt was promoted by the action of clay as a nucleating agent for PBS crystallization. A clear trend did not appear between the intercalation and the extent of promotion of crystallization.

CONCLUSIONS

Nanocomposites based on PBS and organo-modified MMTs (DA-M, ODA-M, ALA-M, LEA-M, and HEA-M) were prepared by melt intercalation and subsequent injection molding. On the basis of TEM and XRD observations, the order of the finer dispersion of

TABLE V
Thermal Properties of PBS and PBS Composites with an Inorganic Content of 3 wt %

	$T_{g,c}$ (°C)	$\Delta H_{g,c}$[a] (J/g)	T_m (°C)	ΔH_m[a] (J/g)	$\Delta H_m - \Delta H_{g,c}$ (J/g)	$T_{m,c}$ (°C)	$\Delta H_{m,c}$[a] (J/g)
PBS	93.9	6.3	114.7	81.9	75.7	76.9	63.0
PBS/MMT	96.7	3.4	114.5	81.1	77.8	81.0	65.2
PBS/DA-M	98.1	6.9	114.6	79.4	72.5	83.2	66.0
PBS/ODA-M	93.2	9.0	114.2	82.4	73.4	82.5	64.7
PBS/LEA-M	98.4	5.4	114.2	77.6	72.2	78.9	63.1
PBS/HEA-M	97.9	3.8	114.0	76.6	72.8	81.0	63.7
PBS/ALA-M	94.1	8.5	114.5	83.9	75.4	83.9	62.2

[a] Per gram of PBS contained in the composite.

the silicate particles in the PBS matrix and of the higher degree of intercalation of the PBS molecule into the silicate layers was determined to be LEA-M, ODA-M > DA-M > ALA-M > HEA-M, MMT. The PBS composites with a higher degree of intercalation showed higher tensile and flexural moduli and lower tensile strength. T_g of the PBS/LEA-M nanocomposite, measured by dynamic viscoelastic measurements, increased with the inorganic content (3–10 wt %), and this indicated that the intercalation of PBS into the galley of silicate layers caused the interference of the molecular motion. The $T_{m,c}$ and ΔH_m values of all the PBS/clay composites were higher than those of PBS, and this indicated that the clay acted as a nucleating agent and promoted the crystallization of PBS.

References

1. Vert, M.; Feijen, J. Biodegradable Polymers and Plastics; Royal Society of Chemistry: London, 1992.
2. Doi, Y.; Fukuda, K. Biodegradable Plastics and Polymers, Proceedings of the Third International Scientific Workshop on Biodegradable Plastics and Polymers, Osaka, Japan, 1993; Elsevier: Amsterdam, 1994.
3. Holemes, P. A. Phys Technol 1985, 16, 32.
4. Avella, M.; Immirzi, B.; Malinconico, M.; Martuscelli, E.; Volpe, M. G. Polym Int 1996, 39, 191.
5. Amass, W.; Amass, A.; Tighe, B. Polym Int 1998, 17, 89.
6. Lehrle, R. S.; Williams, R. J. Macromolecules 1994, 27, 3782.
7. Fujimaki, T. Polym Degrad Stab 1998, 59, 209.
8. Takiyama, E.; Harigai, N.; Hokari, T. Jpn. Pat. H5–70566 (1993).
9. Messersmith, P. B.; Giannelis, E. P. J Polym Sci Part A: Polym Chem 1995, 33, 1047.
10. Jimenez, G.; Ogata, N.; Kawai, H.; Ogihara, T. J Appl Polym Sci 1997, 64, 2211.
11. Pantoustier, N.; Lepoittevin, B.; Alexandre, M.; Kubies, D.; Calberg, C.; Jerome, R.; Dubois, P. Polym Eng Sci 2002, 42, 1928.
12. Chen, G. X.; Hao, G. J.; Guo, T. Y.; Song, M. D.; Zhang, B. H. J Mater Sci Lett 2002, 21, 1587.
13. Lee, S.-R.; Park, H.-M.; Lim, H.; Kang, T.; Li, X.; Cho, W.-J.; Ha, C.-S. Polymer 2002, 43, 2495.
14. Ray, S. S.; Okamoto, K.; Maiti, P.; Okamoto, M. J Nanosci Nanotechnol 2002, 2, 1.
15. Lim, S. T.; Hyun, Y. H.; Choi, H. J. Chem Mater 2002, 14, 1839.
16. Shibata, M.; Takachiyo, K.; Ozawa, K.; Yosomiya, R.; Takeishi, H. J Appl Polym Sci 2002, 85, 129.
17. Shibata, M.; Yosomiya, R.; Ohta, N.; Sakamoto, A.; Takeishi, H. Polym Polym Compos 2003, 11, 359.
18. Shibata, M.; Ozawa, K.; Teramoto, N.; Yosomiya, R.; Takeishi, H. Macromol Mater Eng 2003, 288, 35.
19. Ray, S. S.; Yamada, K.; Ogami, A.; Okamoto, M.; Ueda, K. Macromol Rapid Commun 2002, 23, 943.
20. Pluta, M.; Galeski, A.; Alexandre, M.; Paul, M.-A.; Dubois, P. J Appl Polym Sci 2002, 86, 1497.
21. Chang, J.-H.; An, Y. U.; Sur, G. S. J Polym Sci Part B: Polym Phys 2003, 41, 94.
22. Alexandre, M.; Dubois, P. Mater Sci Eng 2000, 28, 1.
23. Li, X.; Kang, T.; Cho, W.-J.; Lee, J.-K.; Ha, C.-S. Macromol Rapid Commun 2001, 22, 1306.